SECTION 20

VEHICLE AERODYNAMIC CHARACTERISTICS

20.1 SUMMARY

The AS-503 vehicle, as with prior Saturn flights, flew at very low angles-of-attack that did not exceed 2.5 degrees during the period of interest. Because of this a reliable stability and fin load analysis could not be made.

The AS-503 average base differential pressure fell within a predicted band based on AS-502 data even though AS-503 had a 2-degree outboard engine cant and only six valid base pressure measurements whereas AS-502 had eight measurements.

20.2 VEHICLE AXIAL FORCE CHARACTERISTICS

The vehicle axial force characteristics are shown in Figures 20-1 and 20-2. Experience with AS-501, AS-502, and AS-503 flight data has shown that the base differential pressure is a function of altitude and is insensitive to slight Mach number variations. An average base differential pressure which can be used to calculate the base axial force is shown in Figure 20-1. This average was calculated using the six valid base pressure measurements on the AS-503 vehicle whereas eight pressure measurements were used on AS-502. The data for AS-502 and AS-503 show fair agreement. The AS-503 S-IC engines were canted outboard 2 degrees from 20 seconds throughout first stage boost. The small differences that exist are probably a combination of outboard engine cant on AS-503 and the number of base measurements on each flight. Therefore, the effects of engine cant on AS-503 are not readily discernible. The predictions shown are based on AS-502 data. The AS-501 data is also shown, but it should be noted that this vehicle flew with S-IC base flow deflectors installed. A drop off of the data occurred after inboard engine cutoff on each flight.

The forebody axial force coefficient remains a function of Mach number as shown in Figure 20-2. The AS-501 coefficient is greater because of the base flow deflectors. These coefficients are predictions based on wind tunnel data.

The total aerodynamic axial force is then the sum of the base axial force calculated from the base differential pressure and the forebody axial force, as calculated from the forebody coefficient.

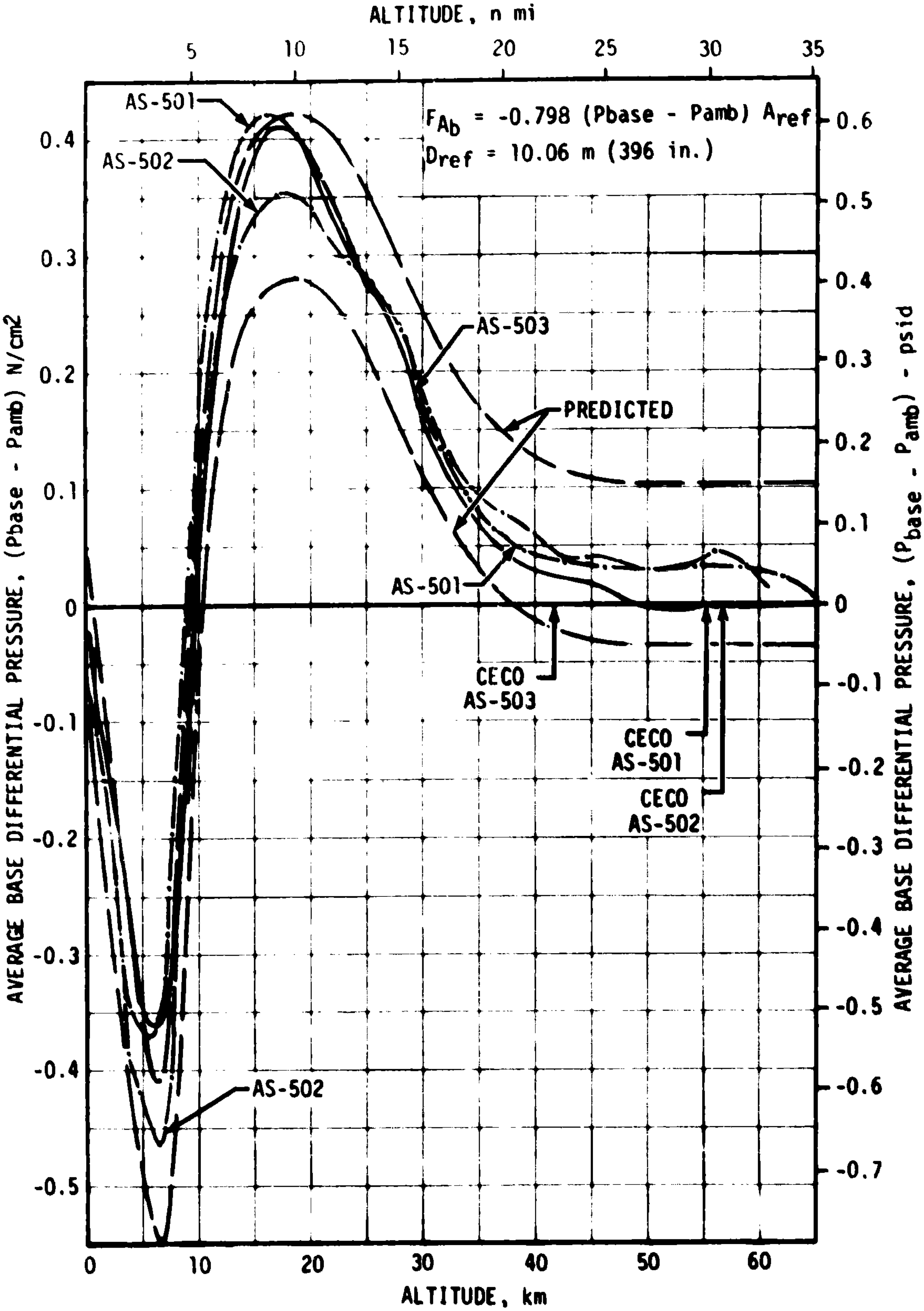

Figure 20-1. Average Base Differential Pressure

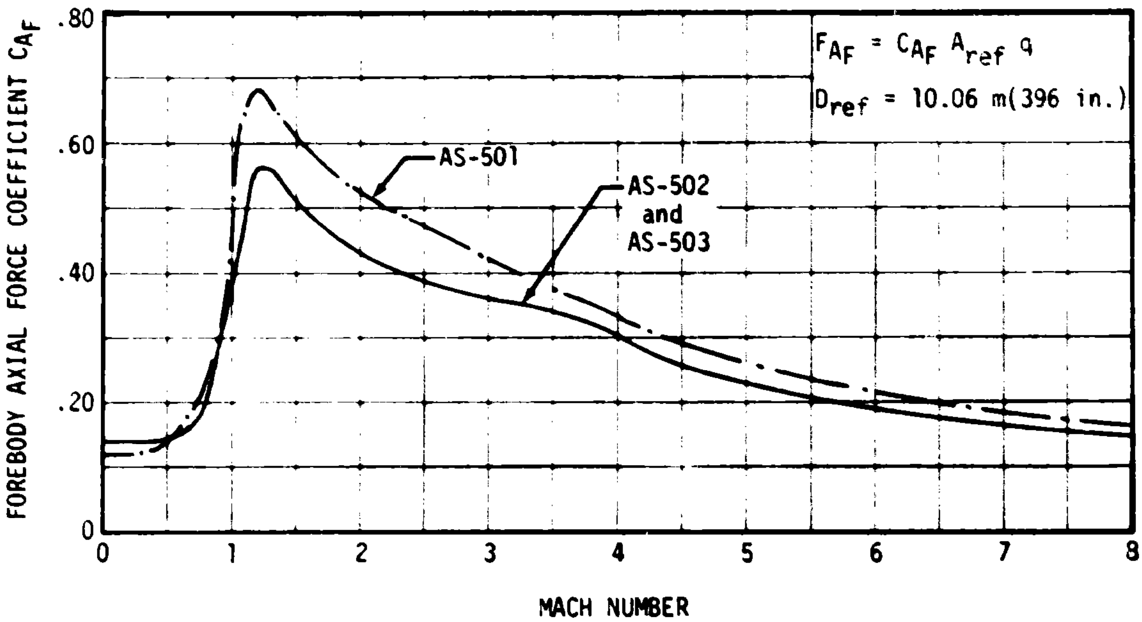

Figure 20-2. Forebody Axial Force Coefficient

20.3 VEHICLE STATIC STABILITY

A reliable evaluation of the static aerodynamic stability characteristics of the AS-503 flight was not possible due to the small vehicle angle-of-attack and resulting small engine deflections.

20.4 FIN PRESSURE LOADING

External static pressures on the S-IC fins were recorded by 16 measurements. Each surface of fins B and D had four measurements located in the same relative position.

Comparisons with predictions or with previous flight data would be misleading because the vehicles flew different angle-of-attack time histories and insufficient low angle-of-attack wind tunnel data are available for accurate predictions. The AS-503 flight angle-of-attack was well below the 10-degree design angle, hence the fin differential pressures were well below design values. Typical fin pressure differentials are shown in Figure 20-3.

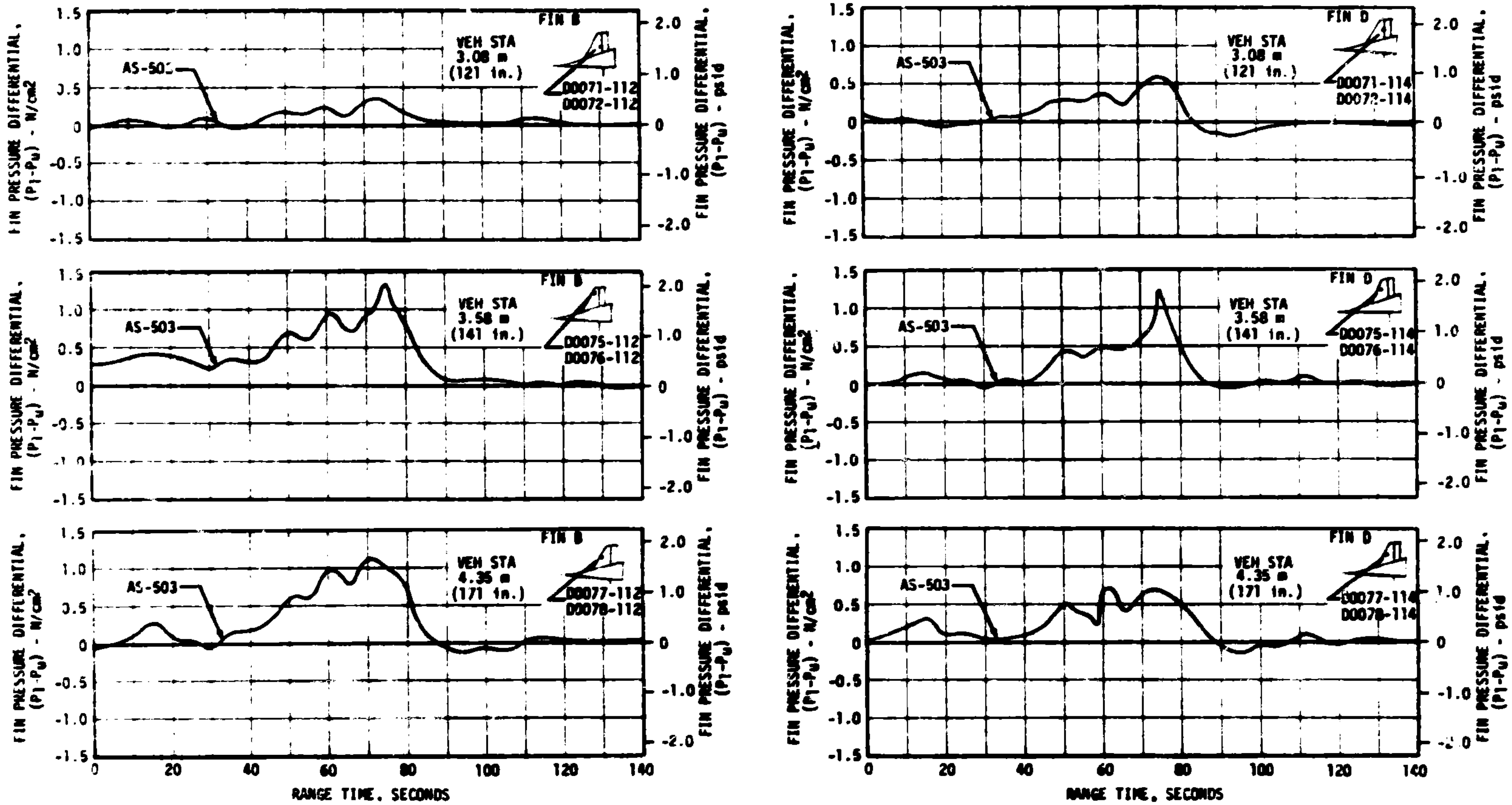

Figure 20-3. S-IC Fin Pressure Differential